

ARTICLE

Received 10 Jan 2012 | Accepted 1 Aug 2012 | Published 11 Sep 2012

DOI: 10.1038/ncomms2039

# TGF $\beta$ induces the formation of tumour-initiating cells in claudin<sup>low</sup> breast cancer

Alejandra Bruna<sup>1,2</sup>, Wendy Greenwood<sup>1,2</sup>, John Le Quesne<sup>1,2</sup>, Andrew Teschendorff<sup>3</sup>, Diego Miranda-Saavedra<sup>4</sup>, Oscar M. Rueda<sup>1,2</sup>, Jose L. Sandoval<sup>1,2</sup>, Ana Tufegdzcic Vidakovic<sup>1,2</sup>, Amel Saadi<sup>1,2</sup>, Paul Pharoah<sup>5,6,7</sup>, John Stingl<sup>1,2</sup> & Carlos Caldas<sup>1,2,6,7</sup>

The role of transforming growth factor-beta (TGF $\beta$ ) in the progression of different molecular subtypes of breast cancer has not been clarified. Here we show that TGF $\beta$  increases breast tumour-initiating cell (BTIC) numbers but only in claudin<sup>low</sup> breast cancer cell lines by orchestrating a specific gene signature enriched in stem cell processes that predicts worse clinical outcome in breast cancer patients. NEDD9, a member of the Cas family of integrin scaffold proteins, is necessary to mediate these TGF $\beta$ -specific effects through a positive feedback loop that integrates TGF $\beta$ /Smad and Rho-actin-SRF-dependent signals. In normal human mammary epithelium, TGF $\beta$  induces progenitor activity only in the basal/stem cell compartment, where claudin<sup>low</sup> cancers are presumed to arise. These data show opposing responses to TGF $\beta$  in both breast malignant cell subtypes and normal mammary epithelial cell subpopulations and suggest therapeutic strategies for a subset of human breast cancers.

<sup>1</sup> Cancer Research UK, Cambridge Research Institute, Li Ka Shing Centre, Cambridge CB2 0RE, UK. <sup>2</sup> Department of Oncology, University of Cambridge, Li Ka Shing Centre, Cambridge CB2 0RE, UK. <sup>3</sup> Medical Genomics Group, Paul O’Gorman Building, UCL Cancer Institute, University College London, London WC1E 6BT, UK. <sup>4</sup> Bioinformatics and Genomics Laboratory, World Premier International (WPI) Immunology Frontier Research Center (IFReC), Osaka University, 3-1 Yamadaoka, Suita, 565-0871 Osaka, Japan. <sup>5</sup> Department of Oncology, Strangeways Research Laboratories, University of Cambridge, Worts Causeway, Cambridge, CB1 8RN, UK. <sup>6</sup> Cambridge Breast Unit, Addenbrooke’s Hospital, Cambridge University, Hospital NHS Foundation Trust and NIHR Cambridge Biomedical Research, Centre, Cambridge CB2 0QQ, UK. <sup>7</sup> Cambridge Experimental Cancer Medicine Centre, Cambridge CB2 0RE, UK. Correspondence and requests for materials should be addressed to A.B. (email: alex.bruna@cancer.org.uk) or to C.C. (email: Carlos.Caldas@cancer.org.uk).

Cancer stem cells or tumour-initiating cells (TICs) have been identified in breast cancer and several other solid tumours<sup>1–5</sup>. Breast TICs (BTICs), identified by their differential ability to generate tumours upon xenotransplantation into immune-deficient mice, were originally characterized as having the EpCAM<sup>+</sup>/CD44<sup>+</sup>/CD24<sup>-/low</sup> phenotype<sup>1</sup>. Human breast cancer is a heterogeneous malignancy with at least five different subtypes (luminal A, luminal B, ERBB2, basal and claudin<sup>low</sup>) described<sup>6–9</sup>. It has been suggested that this heterogeneity results from different breast tumour subtypes originating in cells within distinct compartments of the mammary epithelium<sup>6,10–12</sup>.

Transforming growth factor-beta (TGFβ) has key roles in a variety of cell types and tissues<sup>13</sup>. TGFβ family members bind to a family of membrane receptor serine-threonine protein kinases that activate members of the Smad family of transcription factors (TFs). In cancer, TGFβ has apparently opposite roles, acting both as a tumour suppressor and as a factor that promotes processes such as invasion, metastasis, immune regulation and host–tumour cell interactions<sup>13–15</sup>. In breast cancer, genetic mouse models provide strong support for a tumour suppressor role of epithelial TGFβ signalling in the early stages of mammary gland tumorigenesis<sup>13</sup>. However, both activation and complete depletion of TGFβ signalling enhanced metastasis in mouse models<sup>16–18</sup>. These apparently conflicting reports reveal an incomplete understanding of the role of the TGFβ pathway in breast cancer.

A key role of the TGFβ pathway in regulating both normal and cancer stem cell behaviour in different tissues has recently been described<sup>19–21</sup>. Specifically, a role for the TGFβ pathway in the maintenance of BTICs has been suggested, since EpCAM<sup>+</sup>/CD44<sup>+</sup>/CD24<sup>-/low</sup> cell subpopulations have an active TGFβ signalling pathway<sup>22,23</sup>. However, others have demonstrated that TGFβ suppresses tumorigenesis through inhibition of BTICs in a ER-negative (ER<sup>-</sup>) breast cancer model<sup>24</sup>. In the experiments described here, we aimed to reconcile these observations by taking into account breast cancer heterogeneity. We have examined TGFβ effects on BTICs and demonstrate TGFβ has opposing effects on different types of breast cancer. Mechanistically we show that TGFβ/Smad signalling converges with active SRF to increase BTIC numbers in claudin<sup>low</sup> cell lines through the regulation of a specific gene expression program (TβSC-A). Induction of NEDD9 is necessary to establish a positive feedback loop that links TGFβ/Smad and Rho-actin-SRF signals, which meet at regulatory regions within TβSC-A genes necessary for BTIC activity. Similar opposing effects were observed in normal human mammary epithelial cell subpopulations revealing conserved responses to TGFβ in both malignant and normal mammary epithelial cells.

## Results

**TGFβ differentially regulates mammosphere-initiating cell (MS-IC) numbers.** To study the effects of TGFβ on stem cell-like traits, we cultured 11 distinct breast cancer cell lines in suspension as floating spheres (mammospheres) as previously described (Fig. 1a; Supplementary Table S1)<sup>25</sup>. Mammosphere cultures were found to be selectively enriched for tumour-initiating cells (TICs) by limiting dilution transplants into the mammary fat pads of NOD/SCID interleukin-2 receptor gamma chain null (Il2rg<sup>-/-</sup>) (NSG) mice, when compared with adherent 2D (Table 1). The self-renewal activity and proliferation capacity of cells within the first-generation mammosphere culture (M1) were assayed using MS-IC and colony-forming cell (CFC) assays, respectively<sup>25,26</sup> (Fig. 1a). We observed that TGFβ decreased the number of both MS-ICs and CFCs in MCF7, CAMA1, SKBR3, SKBR7, HCC1954 and SUM149 cultures. In contrast, TGFβ treatment increased the number of MS-ICs and CFCs in PMC42, MDA-MB-231, BT549 and SUM159 cultures (Fig. 1b; Supplementary Fig. S1). TGFβ treatment had no effect in T47D cultures. A TGFβ receptor I inhibitor (SB) counteracted

TGFβ-mediated changes in MS-IC and CFC numbers (Fig. 1b and Supplementary Fig. S1).

We observed a correlation between increased self-renewal activity in response to TGFβ with the claudin<sup>low</sup> signature<sup>9</sup> showing cells with this phenotype respond to TGFβ similarly and in an opposite way compared with other molecular subtypes (Supplementary Table S1, Supplementary Fig. S1 and Supplementary Methods).

To investigate the effect of TGFβ on the self-renewal properties of TICs, we transplanted M1 single-cell suspensions from ER<sup>-</sup> cell lines prototypic of the opposing effects of TGFβ on MS-IC self-renewal (HCC1954-basal and MDA-MB-231-claudin<sup>low</sup>) at limiting dilutions into the mammary fat pads of NSG mice (Fig. 1a). In HCC1954 M1 cultures, TGFβ mediated a fourfold decrease in the total number of TICs (Fig. 1c; Table 1). In contrast, in MDA-MB-231 M1 cultures TGFβ induced a fivefold increase in the absolute number of TICs (Fig. 1c; Table 1).

We next modulated the TGFβ pathway in HCC1954 and MDA-MB-231 cells by lentiviral transduction of a constitutive active mutant TGFβ1 (Tβ1CA) or a dominant negative mutant of type II TGFβ receptor (TβRII-ΔCyt) (Supplementary Methods)<sup>27,28</sup>. TGFβ pathway activation levels were measured by western blotting for p-Smad2 (Supplementary Fig. S1). MDA-MB-231-Tβ1CA showed increased MS-IC and BTIC numbers (compared with MDA-MB-231-vector control) (Fig. 1d; Table 1). HCC1954-Tβ1CA displayed impaired mammosphere growth precluding propagation for further analysis. The TGFβ effects on MS-IC and BTIC numbers were counteracted by the expression of TβRII-ΔCyt in both cell lines (Fig. 1d; Table 1).

Recently, TGFβ treatment of immortalized human mammary epithelial cells has been shown to induce epithelial-to-mesenchymal transition (EMT) and increase the number of CD44<sup>+</sup>/CD24<sup>-/low</sup> cells, a phenotype of breast normal and cancer stem cells<sup>1,22</sup>. We asked whether the opposing responses to TGFβ in BTIC activity were associated with EMT and/or CD44<sup>+</sup>/CD24<sup>-/low</sup> phenotypes. TGFβ increased the expression of mesenchymal markers (vimentin, fibronectin, Slug and FOXC2) and decreased the expression of the epithelial marker E-cadherin and increased the number of CD44<sup>+</sup>/CD24<sup>-/low</sup> cells in the basal cell line HCC1954 (Fig. 1e,f). The claudin<sup>low</sup> cell line, MDA-MB-231, expresses mesenchymal markers and we did not observe significant changes on their expression upon TGFβ treatment, yet in these cells, TGFβ also increased the number of CD44<sup>+</sup>/CD24<sup>-/low</sup> cells (Fig. 1f and data not shown). These data show TGFβ-mediated induction of EMT and CD44<sup>+</sup>/CD24<sup>-/low</sup> phenotypes are separable from its effects on BTICs.

## TGFβ regulates normal human breast epithelial subpopulations.

We next asked whether TGFβ would have similar opposing effects in distinct normal breast epithelial cell subpopulations, which are the putative cells of origin of the different breast cancer subtypes. To study the effects of the TGFβ pathway on normal human breast epithelial cell subpopulations, we FACS sorted cells from human reduction mamoplasties using CD49f and EpCAM antibodies (Fig. 2a)<sup>29,30</sup>. To assess baseline TGFβ pathway activity in these subpopulations we performed qRT-PCR and show that TGFβ downstream targets (*Smad7*, *NEDD9* and *SERPINA*) were expressed exclusively in the basal compartment (CD49f<sup>+</sup>/EpCAM<sup>neg/low</sup>, fraction B in Fig. 2a), a population that contains myoepithelial cells, myoepithelial-restricted progenitors and mammary stem cells (MaSCs) (Fig. 2b). The expression of these transcripts was undetectable in the non-clonogenic ER<sup>+</sup> luminal cell population (CD49f<sup>-</sup>/EpCAM<sup>+</sup>, fraction C) or the luminal progenitor population (CD49f<sup>+</sup>/EpCAM<sup>+</sup>, fraction A). Recently, CD49f<sup>+</sup>/EpCAM<sup>neg/low</sup>, but not CD49f<sup>+</sup>/EpCAM<sup>+</sup> cells, have been shown to express high levels of nuclear Smad2<sup>21</sup>. Together with our data, this confirms the presence of an active TGFβ pathway in the basal but not in the luminal progenitor compartment. We next determined the effects of ectopic

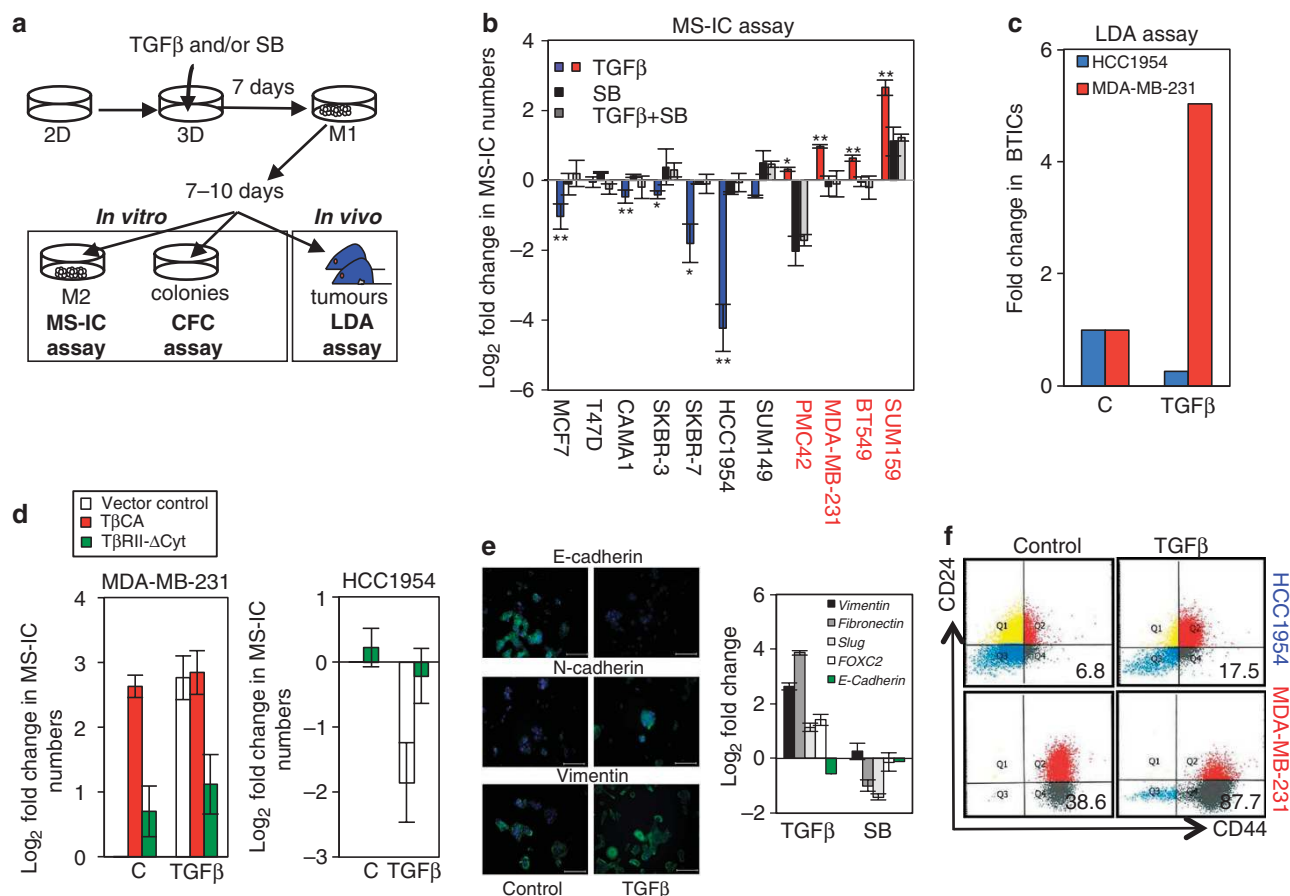


**Figure 1 | Effects of TGFβ pathway activation on human BTICs.** (a) Schematic representation of the *in vitro* and *in vivo* experimental approaches that were used in combination to study TGFβ regulation of BTIC behaviour. (b) MS-IC assay. Bar chart shows log<sub>2</sub> fold changes of M2 mammosphere numbers (which is a read-out of MS-ICs in the M1 cultures) in treated compared with untreated cultures. Error bars represent ±s.d. of at least three independent experiments. \*\*TGFβ-treated versus untreated cultures,  $P < 0.01$ . \*TGFβ-treated versus untreated cultures,  $P < 0.05$  (Student's *t*-test) (c) LDA assay: different doses of single cells from HCC1954 and MDA-MB-231 M1 mammospheres left untreated or treated with TGFβ (2.5 ng ml<sup>-1</sup>) for 7 days, as indicated, were implanted in the mammary fat pad of NSG mice at limiting dilutions. Bars represent fold change in total number of BTICs in TGFβ-treated M1 as compared with untreated M1 cultures. (d) Same number of single cells from MDA-MB-231- and HCC1954-expressing lenti-HIV-ZsGreen control (vector control), lenti-Tβ1CA (TβCA) or lenti-TβRII-ΔCyt (TβRII-ΔCyt) were grown as M1 mammospheres and left untreated or treated with TGFβ (2.5 ng ml<sup>-1</sup>) for 7 days as indicated and then processed as in (b). Bar chart shows log<sub>2</sub> fold changes of MS-ICs in M1 mammospheres compared with vector control untreated M1 cultures. Error bars represent ±s.d. of at least three independent experiments. (e) Immunofluorescence analysis for the expression of E-cadherin, N-cadherin and vimentin in HCC1954 cells grown for 7 days as M1 mammospheres in the absence or presence of TGFβ and then for 24 h in attached conditions. Scale bars, 250 μm (left panel). qRT-PCR assays to assess expression of the indicated transcripts in HCC1954 M1 mammospheres treated with TGFβ (2.5 ng ml<sup>-1</sup>) or of SB (10 μM) for 4 days. Error bars represent ±s.d. of three independent experiments (right panel). (f) FACS plots of CD44-FITC- and CD24-PE-stained HCC1954 and MDA-MB-231 M1 mammospheres left untreated or treated with TGFβ (2.5 ng ml<sup>-1</sup>) for 7 days. Numbers indicate the percent of CD44<sup>+</sup>/CD24<sup>-/low</sup> population.

activation of the TGFβ pathway in these subpopulations using an *in vitro* CFC assay. We observed TGFβ treatment decreased the number of colonies generated from the CD49f<sup>+</sup>/EpCAM<sup>+</sup> subpopulation and increased the number of colonies generated from the CD49f<sup>+</sup>/EpCAM<sup>neg/low</sup> cell subpopulation (Fig. 2c). Similar results were obtained from the analogous mouse epithelial cell subpopulations (Supplementary Fig. S2). However, TGFβ decreased total cell numbers in both compartments (Supplementary Fig. S2). We noted the few colonies derived from TGFβ-treated CD49f<sup>+</sup>/EpCAM<sup>+</sup> cells were scattered and of mesenchymal appearance, morphologically identical to the colonies generated from the basal compartment (Fig. 2d<sup>29</sup>). Consistently, these colonies expressed the basal marker cytokeratin 14 (Fig. 2e).

To directly investigate TGFβ effects on the number of progenitors and MaSCs, we used a xenotransplantation-based protocol previously described for the quantification of human mammary

cells with *in vivo* regenerative capacity<sup>30,31</sup>. Briefly, flow-sorted human breast epithelial cells were exposed to TGFβ or SB for 3 h. Next, the cells were embedded into collagen gels along with supportive fibroblasts, and the gels transplanted under the renal capsule of estrogen- and progesterone-supplemented NSG mice. After 4 weeks, the gels were removed and dissociated, and the liberated cells were seeded into secondary CFC assays (as depicted in Fig. 2a). TGFβ treatment, *in vivo* resulted in a decrease in the clonogenic output (CFCs/outgrowth) of CD49f<sup>+</sup>/EpCAM<sup>+</sup> and an increase in CD49f<sup>+</sup>/EpCAM<sup>neg/low</sup> cells, compared with their SB-treated counterparts (Fig. 2f,g). Morphologically<sup>32</sup>, we observed a similar trend in secondary CFCs: colonies derived from TGFβ-treated luminal progenitor outgrowths were exclusively basal, whereas SB-treated outgrowths generated predominantly luminal colonies (Fig. 2g,h). Altogether these results show TGFβ differentially regulates human normal mammary epithelial cell subpopulations independently

**Table 1 | Frequencies and absolute number of BTICs in mammosphere and adherent 2D cultures.**

Cell lines	Cell dose								f	95% CI	P	(Total cell number in M1), absolute number of BTICs
	1	5	10	20	25	30	50	100				
HCC1954		3/4	4/4	4/4		4/4	4/4	4/4	1:3	1:1-1:8	0.9984	(600,000), 200,000
HCC1954-TGFβ		0/4	2/4	3/4		4/4	4/4	4/4	1:14	1:7-1:26	0.7956	(750,000), 53,571
MDA-MB-231	0/4	2/4	1/4	0/4		2/4	4/4		1:33	1:17-1:65	0.1092	(295,000), 8,939
MDA-MB-231-TGFβ	0/4	0/4	0/4	1/4		3/4	2/2		1:40	1:18-1:87	0.4619	(1,800,000), 45,000
MDA-MB-231-TGFβ+Y		0/4	0/4	0/4		0/4	0/4	1/4	1:809	1:116-1: 5627	0.9373	(1,320,000), 1,630
MDA-MB-231-vector control	0/4	2/4	0/4		1/4		3/4		1:43	1:19-1:98	0.092	(500,000), 11,627
MDA-MB-231-TβRII-ΔCyt	1/4	1/4	2/4		1/4		4/4		1:22	1:11-1:46	0.0846	(305,000), 13,864
MDA-MB-231-TβRII-ΔCyt- TGFβ	0/4	2/4	1/4		1/4		1/4		1:62	1:39-1:101	0.0170*	(800,000), 12,903
MDA-MB-231-TβCA	0/4	0/4	0/4		2/4		2/4		1:70	1:26-1:188	0.7843	(1,400,000), 20,000
MDA-MB-231-Φ-TGF β	0/4	0/4	0/4		1/4		3/4		1:67	1:41-1:109	0.7568	(850,000), 12,687
MDA-MB-231-sh1NEDD9-TGF β	0/4	0/4	0/4		0/4		0/4		>1:364			(950,000), <2,610
MDA-MB-231-sh2NEDD9-TGF β	0/4	0/4	0/4		0/4		2/4		1:156	1:40-1:605	0.7105	(1,050,000), 6,731
Cell lines	Cell dose						f	95% CI	P	(Total cell number in a 10-cm cell-culture dish), absolute number of BTICs		
	10	50	100	200	300	500						
HCC1954 (2D)	0/4	0/4	0/4	0/4	0/4	0/4	>1:3,784	1:26,356-1:543	0.9504		(1,400,000), <3,700	
MDA-MB-231(2D)	0/4	0/4	0/4	0/4	0/4	2/4	1:2,060	1:8,035-1:528	0.659		(2,600,000), 12,621	

Cells from the indicated cell lines were plated at the same density (50,000 cells per ml) in 4 ml of supplemented MEBM and grown as M1 mammospheres for 7 days. HCC1954 and MDA-MB-231 cell lines were also grown in a 10 cm cell-culture dish in 2D in RPMI and DMEM 10% FBS, respectively. Single-cell suspensions from these cultures were implanted into the mammary fat pad of NSG mice. Results show the number of tumours per number of implanted mammary fat pads. BTIC frequencies per transplanted populations (f) and upper and low limits (95% CI) were calculated by limiting dilution analysis. Consistency of the fit of the data according to a single-hit model is indicated by P-values (Chi-square) >0.05 (P) (all conditions except one \* complied). Total cell number in the mammosphere cultures 7 days after and their calculated absolute number of BTICs is shown.

of its cytostatic effects (which are similar in both): it decreases luminal progenitor proliferation and clonogenic capacity and alters their phenotype, and it increases the clonogenic output of MaSC/basal progenitors within the basal compartment.

**Similar TGFβ signalling in different BTICs.** We next determined whether the differential effects of TGFβ on BTICs were due to intrinsic differences in the activity of the TGFβ signalling pathway. TGFβ receptors were functional, as shown by increased p-Smad2 levels after TGFβ treatment in all cell lines except T47D. T47D cells do not express TβRII making them unresponsive to TGFβ<sup>33</sup>. Western blotting revealed that total levels of Smads were variable among cell lines, although no significant differences were found between cells with increased and cells with decreased BTIC activity upon TGFβ treatment (Supplementary Fig. S3). To demonstrate whether the TGFβ effects on BTICs are Smad-dependent, we used short interfering RNA (siRNA) to knock down Smad2, Smad3, Smad2 and 3 together and Smad4, and this greatly impaired the effects of TGFβ on M1 on both HCC1954 and MDA-MB-231 cells (Fig. 3a; Supplementary Fig. S3). Using a reporter assay, we also confirmed that Smads were similarly transcriptionally active in M1 from both TGFβ-treated cell lines (Fig. 3b).

We noted that pathway activation was sustained during the M1 culture and persisted 7 days after the single dose of recombinant TGFβ was added to the culture on day 1 (Supplementary Fig. S3), suggesting induction of a positive autocrine TGFβ signalling feedback loop. To test this hypothesis, MDA-MB-231 cells, untreated or treated with recombinant TGFβ bound to biotin (TGFβB) were grown in mammosphere medium and supernatants collected at days 1, 2, 5 and 7. Exogenous TGFβB was removed using magnetic streptavidin-beads, and levels of TGFβ1, 2 and 3 in the supernatant were

measured using a multiplex immunoassay. The levels of endogenously secreted TGFβ1 and 2 (TGFβ3 levels were undetectable) increased throughout the 7 days of the experiment (Supplementary Fig. S3 and Supplementary Methods). These results suggest that the persistent pathway activation in TGFβ-treated M1 mammospheres is due to a positive feedback loop of autocrine TGFβ signalling. As we observe similar levels of p-Smad2 upon a single dose of TGFβ in M1 derived from cell lines with opposing responses to TGFβ, autocrine activation of TGFβ production and subsequent sustained TGFβ pathway activation in mammosphere cultures is not related to the differential TGFβ effects on BTICs.

In summary, these results demonstrate that the opposing effects of TGFβ on BTIC regulation are not explained by differences in the activity of TGFβ receptors, Smad activity or the positive feedback loop of autocrine TGFβ.

**A TGFβ expression signature for self-renewal of MS-ICs.** As the differential effects of TGFβ on BTICs from distinct breast cancer cell lines are Smad-dependent, and could not be assigned to differences in Smad transcriptional activity, we hypothesized that the differences could result from distinct TGFβ/Smad-specific transcriptional programs. We profiled, using microarrays, M1 cultures from two cell lines prototypic of TGFβ-mediated decrease (MCF-7 and HCC1954) and two cell lines prototypic of TGFβ-mediated increase (MDA-MB-231 and BT549) in BTIC activity (Fig. 1b) (Accession in ArrayExpress E-MTAB-516 and E-MTAB-1190). We focused on genes differentially regulated (1% false discovery rate (FDR) and >1 log-fold-change) by TGFβ versus SB. There were 114 TGFβ-specific genes common and unique to MCF-7 and HCC1954 (TGFβ-specific cancer stem cell signature-B or TβSC-B) and 130 TGFβ-specific genes common and unique to MDA-MB-231 and BT549

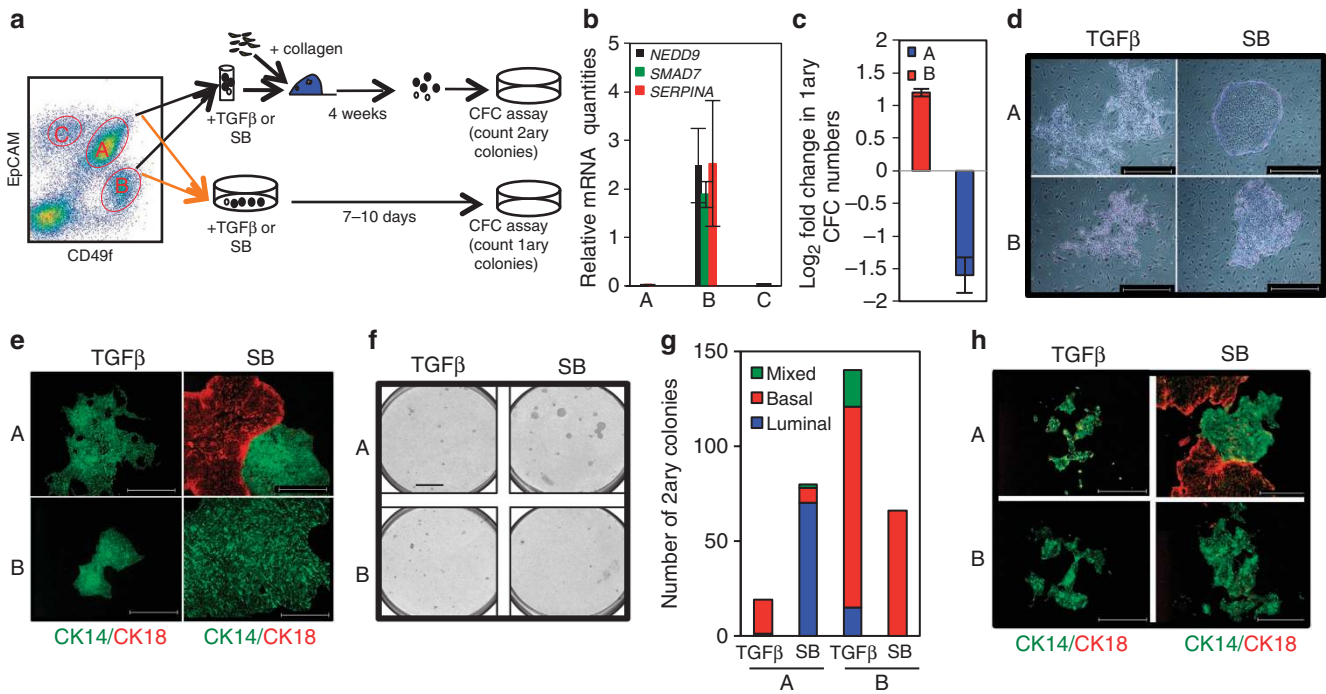


**Figure 2 | TGFβ effects on normal human mammary epithelium.** (a) FACS profile of human mammary epithelial cell preparations (depleted of CD45<sup>+</sup> and CD31<sup>+</sup> cells) showing the gates used to select normal human mammary epithelial cell subfractions; A: CD49f<sup>+</sup>/EpCAM<sup>+</sup>, B: CD49f<sup>+</sup>/EpCAM<sup>neg/low</sup> and C: CD49f<sup>-</sup>/EpCAM<sup>+</sup>, and schematic representation of the *in vitro* and *in vivo* experimental approaches that were used to obtain primary and secondary CFCs, respectively. (b) qRT-PCR of the indicated transcripts in epithelial sub fractions as depicted in (a). Expression was normalized against beta-2-microglobulin and displayed as arbitrary units. Error bars represent  $\pm$ s.d. of three independent experiments. (c) TGFβ (2.5 ng ml<sup>-1</sup>) was added (at day 0) to flow-sorted subfractions as depicted in (a) and plated at clonogenic densities in the presence of feeder cells (irradiated fibroblasts) in collagen-coated plates for 7–10 days. Colonies were stained with Giemsa and counted. Results are represented as the log<sub>2</sub> fold changes of primary colonies (or CFCs) in TGFβ-treated compared with untreated cells. Error bars represent  $\pm$ s.d. of three independent experiments. (d) Microscopy images of Giemsa-stained primary colonies from CFC assays of flow-sorted TGFβ- (2.5 ng ml<sup>-1</sup>) or SB-(10 μM)-treated cells from fractions A or B. Scale bars, 1 mm. (e) Immunostaining for expression of cytokeratin 14 (green) and cytokeratin 18 (red) of primary colonies from CFC assays of flow-sorted TGFβ- (2.5 ng ml<sup>-1</sup>) or SB (10 μM)-treated mammary epithelial subpopulation A and B. Scale bars, 1 mm. (f) Representative images of secondary colonies of TGFβ- (2.5 ng ml<sup>-1</sup>) or SB (10 μM)-treated mammary epithelial subpopulation A and B. Scale bars, 1 cm. (g) Bar chart showing number and type (according to their morphology) of secondary colonies of a representative secondary CFC assay of TGFβ- and SB-treated mammary epithelial fractions A and B. (h) Immunofluorescence using antibodies against cytokeratin 14 (CK14) and cytokeratin 18 (CK18) of representative colonies derived from (g). Scale bars, 1 mm

(TGFβ-specific cancer stem cell signature-A or TβSC-A) (Fig. 3c; Supplementary Data 1).

Gene set enrichment analysis (GSEA) on these signatures using the Molecular Signatures Database<sup>34</sup> showed both TβSC-A and -B signatures are TGFβ-specific signatures (Supplementary Data 2). Moreover, the most significantly enriched gene list in TβSC-A was a signature for stemness (53-gene overlap,  $P < 10^{-28}$ , FDR < 0.05), which was only marginally enriched in TβSC-B (13-gene overlap,  $P < 10^{-4}$ , FDR < 0.05) (Supplementary Data 2). Analysis using MetaCore data mining technology, which has previously been used in the field<sup>23</sup>, showed one of the most significantly enriched pathways in TβSC-A was EMT in cancer cells ( $P < 0.0003$ , FDR < 0.05) (Supplementary Table S2; Supplementary Fig. S3). To explore these signatures further, we used a recently derived protein–protein interaction subnetwork characterizing pluripotency and stemness (the ‘Pluri-Net’)<sup>35</sup> and found it was preferentially upregulated only in TβSC-A (Fig. 3d). Interestingly, using our Metabarc data set<sup>36</sup>, we observed TβSC-A upregulated genes are enriched in human claudin<sup>low</sup> tumours (which are the most undifferentiated subtype of breast cancer) compared with the other molecular subtypes (Fig. 3e).

BTIC numbers have been suggested to vary between breast cancers, and correlate with clinical aggressiveness<sup>37</sup>. We hypothesized that the TβSC-A signature, as linked to increase in BTIC numbers, would correlate with clinical outcome. Kaplan–Meier analysis of

tumours with the 25% extreme high and low correlation values with TβSC-A, showed this synexpression signature was associated with time to distant metastasis in both ER<sup>-</sup> and ER<sup>+</sup> tumours. In contrast, TβSC-B showed no significant associations (Fig. 3f; Supplementary Methods). We further assessed p-Smad2 expression by immunohistochemistry as a readout of canonical TGFβ pathway activation in 1714 breast cancer cores on TMAs and saw no significant correlation with overall survival in either ER<sup>-</sup> or ER<sup>+</sup> breast cancer patients (Supplementary Fig. S3 and Supplementary Methods). Thus, canonical TGFβ pathway activation levels (measured by p-Smad2) cannot be used as a prognostic marker in breast cancer, contrasting with synexpression signature TβSC-A, which confers poor prognosis, further strengthening its biological significance.

**SRF and Smad signalling increase BTIC numbers.** The TGFβ-specific synexpression signatures represent two distinct cellular context-dependent TGFβ-induced gene responses and are likely to be jointly controlled by a specific Smad-cofactor (TF) combination<sup>13</sup>. To identify these TFs, we used the regulatory network approach (Fig. 4a) that compares the differential expression levels of predicted TF targets to the non-targets in TβSC-A and TβSC-B<sup>38,39</sup>. This revealed that SRF (serum response factor) targets were the most significantly differentially expressed in TβSC-A ( $P < 0.01$ , *t*-test). Predicted targets of SRF were not differentially

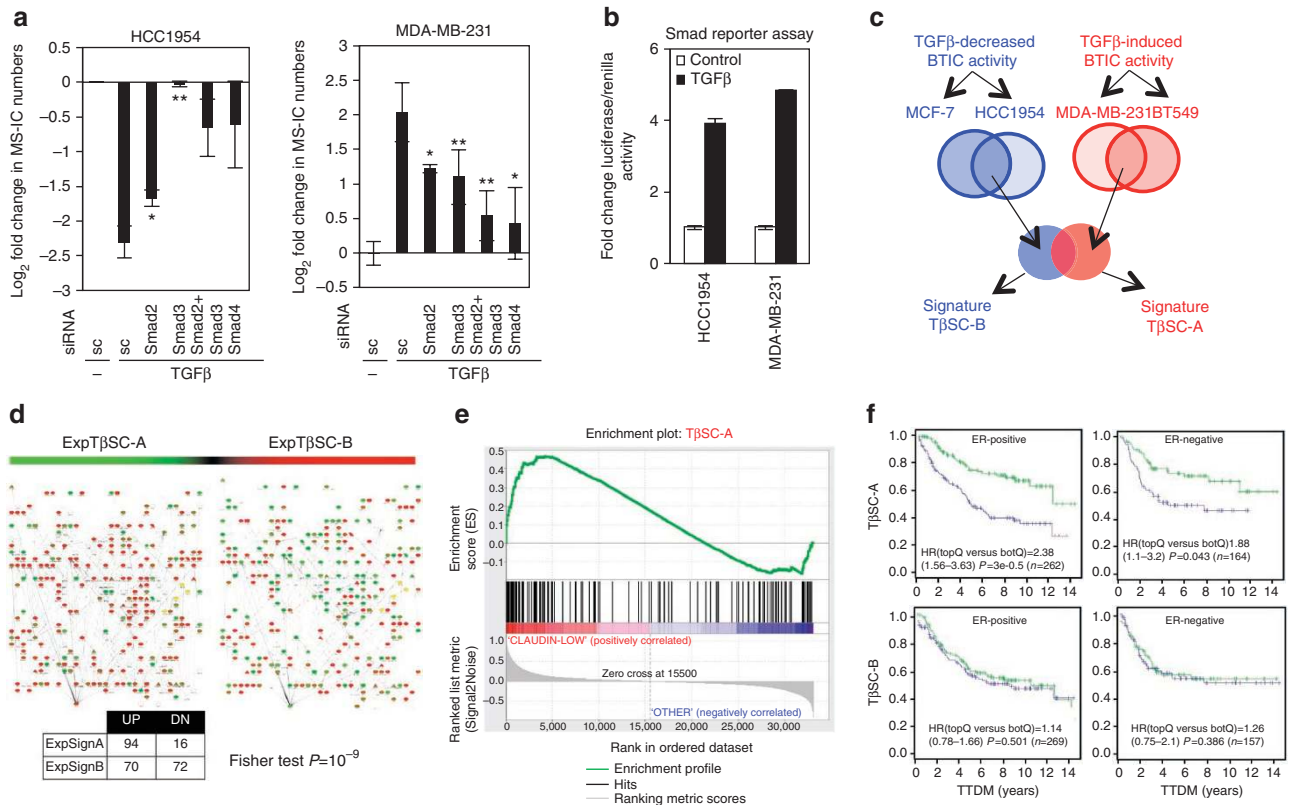


**Figure 3 | TβSC-A is prognostic in breast cancer.** (a) Bar chart shows log<sub>2</sub> fold change of MS-ICs in TGFβ-treated compared with untreated HCC1954 and MDA-MB-231 M1 cultures transfected with the indicated siRNAs. Data represents the mean ± s.d. of three independent experiments. \*\*TGFβ-treated scramble siRNA (sc) cultures versus TGFβ-treated siSmad cultures,  $P < 0.01$ . \*TGFβ-treated scramble siRNA (sc) cultures versus TGFβ-treated siSmad cultures,  $P < 0.05$  (Student's *t*-test). (b) Luciferase activity of untreated (Control) or TGFβ-(2.5 ng ml<sup>-1</sup>) treated 4-day M1 mammospheres from HCC1954 and MDA-MB-231 transfected (at day 2) with a Smad reporter vector (CAGA<sub>12</sub>-Luc) normalized to pGL-SV40 renilla transfection control. Results are expressed as fold change from untreated cultures. Data represents the mean ± s.d. of three independent experiments. (c) Schematic representation of the experimental design used to derive TGFβ-specific signatures. Blue- and red-line Venn diagrams represent differentially expressed genes (DEG) in TGFβ- versus SB-treated M1 mammospheres. TβSC-A and TβSC-B signatures were obtained from the list of DEG common and unique to MDA-MB-231 and BT549 (red circle) or common and unique to MCF-7 and HCC1954 (blue circle), respectively. (d) Heat-map-like (red represents upregulated, green represents downregulated) visualization of 'Plurinet' genes for expression data from ExpTβSC-A and ExpTβSC-B. (e) Enrichment plot of upregulated genes from TβSC-A shows a significant enrichment (FDR  $q$ -value: 0.05) in the claudin<sup>low</sup> subtype (104 tumours) versus the rest of the Metabric tumours (893)<sup>36</sup>. The top panel displays the enrichment score. The middle panel shows the position of the genes in the signature in the ranked list of all the genes in the microarray (33,075). The lower panel displays the value of the signal to noise ratio, a measure of the correlation of each gene with the claudin<sup>low</sup> subtype. (f) Kaplan-Meier estimates of time to distant metastasis (TTDM) for top (blue or topQ) and low (green or botQ) quartiles of TβSC-A and TβSC-B activation levels as measured by Spearman rank correlation. Hazard ratio (HR), 95% confidence interval,  $P$ -values (Wald test) and numbers of patients are also included. Values of a stratified Cox-regression model where all samples are included, and stratification is done according to cohort are: TβSC-A-ER<sup>+</sup>: HR = 1.319 (1.15-1.5)  $P = 7e-05$   $n = 532$ ; TβSC-A-ER<sup>-</sup>: HR = 1.19 (1.01-1.41)  $P = 0.043$   $n = 328$ ; TβSC-B-ER<sup>+</sup>: HR = 1.07 (0.93-1.22)  $P = 0.366$   $n = 532$ ; TβSC-B-ER<sup>-</sup>: HR = 1.07 (0.93-1.22)  $P = 0.366$   $n = 532$ .

expressed in TβSC-B, suggesting that the regulation of SRF targets in response to TGFβ is specific to claudin<sup>low</sup> cell lines (Fig. 4a; Supplementary Fig. S4 and Supplementary Data 3).

To investigate this further, we performed MS-IC assays in siSRF-MDA-MB-231 cells and observed a 50% reduction in TGFβ-mediated increase in MS-IC numbers compared with control siRNA-transfected cells. In HCC1954, SRF knockdown did not affect TGFβ-mediated decrease in self-renewal of MS-ICs (Fig. 4b,c).

We next wanted to investigate whether the SRF-dependent increase in claudin<sup>low</sup> BTIC activity in response to TGFβ relies on Rho-actin-MRTF (myocardin-related TFs) signals, as SRF activity is controlled by the Rho-actin pathway in MDA-MB-231 cells<sup>40</sup>. We observed TGFβ treatment increased Rho activity in MDA-MB-231 but not in HCC1954 M1 mammospheres (Supplementary Fig. S4). Indeed, siRNAs against Rho-A, Rho-C and Rho-actin-MRTF-SRF downstream targets (*Fos*, *CTGF* and *Cyr61*)<sup>40</sup> specifically abrogated TGFβ-mediated effects in MS-IC numbers in MDA-MB-231, but

not in HCC1954 (Fig. 4b,c and Supplementary Fig. S4). Furthermore, inhibition of the Rho effector ROCK (Rho-kinase) using the inhibitor Y-27632, strongly inhibited the increase in MS-IC and BTIC numbers upon TGFβ treatment (Fig. 4d,e; Table 1). Treatment with actin-modifier drugs Latrunculin A and B (LA and LB), which inhibit SRF activation through MRTFs, partially blocked TGFβ-mediated increase in MS-IC numbers (Fig. 4f). Altogether, these results show Rho-actin-MRTF-SRF signalling is necessary for TGFβ-mediated increase in BTIC activity exclusively in claudin<sup>low</sup> cells.

**MRTF-SRF and Smad induce NEDD9 in claudin<sup>low</sup> cancer cells.** Our transcriptomic approach showed the gene *NEDD9* (neural precursor cell expressed developmentally downregulated 9) to be one of the top ten differentially expressed genes in the claudin<sup>low</sup> cell lines, but not in others (Supplementary Data 1). This result was validated by qRT-PCR (Supplementary Fig. S5). Significantly,

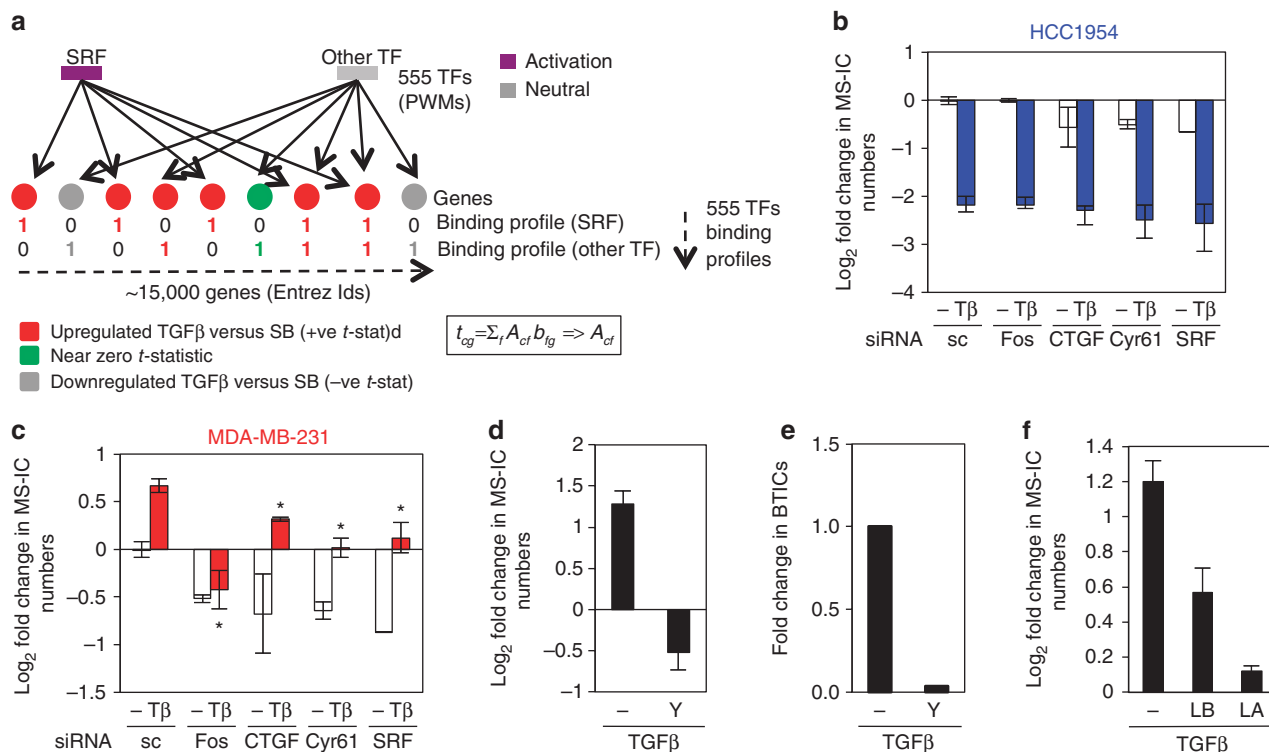


**Figure 4 | MRTF-SRF signalling mediates TGFβ increased in BTIC self-renewal.** (a) Regulatory network analysis used to infer differential activity of position weight matrices (PWMs) between two conditions (TGFβ versus SB) in a given cell line (c). The regularized *t*-statistics of differential expression of ~15,000 genes between the two conditions (*t*) is regressed against the binding profiles, (b), of 555 PWMs ( $f=1, \dots, 555$ , coded as 1s-bound and 0s-unbound) to infer differential activity of PWMs. Differential activity estimates are provided by the regression coefficients (*A*). (b) Bar chart shows log<sub>2</sub> fold change of MS-ICs in M1 cultures of untreated (-) and TGFβ-treated (Tβ) HCC1954 (b) and MDA-MB-231 (c) transfected with siRNAs to knockdown *Fos*, *CTGF*, *Cyr61* and *SRF* as indicated, compared with scramble siRNA (sc)-untreated M1 cultures. Data represents the mean ± s.d. of three independent experiments. \*TGFβ-treated scramble siRNA (sc) versus TGFβ-treated siRNA (*Fos*, *CTGF*, *Cyr61* and *SRF*),  $P < 0.05$  (Student's *t*-test). (d) Bar chart shows log<sub>2</sub> fold change of MS-ICs in TGFβ-treated MDA-MB-231 M1 cultures in the presence of 25 μM Y-27632 compared with M1-untreated cultures (-). Error bars represent ± s.d. of three independent experiments. (e) LDA assay using different doses of single cells derived from MDA-MB-231 M1 mammospheres cells left untreated or treated with TGFβ (2.5 ng ml<sup>-1</sup>) in the absence (-) or presence of Y-27632 for 7 days. Bars represent fold change in total number of BTICs in M1 cultures as compared with M1 untreated cultures. (f) Bar chart shows log<sub>2</sub> fold change of MS-ICs in TGFβ-treated MDA-MB-231 M1 cultures in the absence (-) or presence of 0.5 μM latrunculin B (LB) or of 0.4 μM latrunculin A (LA) compared with untreated cells. Error bars represent ± s.d. of at least three independent experiments.

*NEDD9* was also overexpressed in claudin<sup>low</sup> tumours compared with other subtypes of breast cancer (Supplementary Fig. S5). We next confirmed *NEDD9* is a Smad and SRF target with a siRNA approach. SRF and Smad downregulation in M1 MDA-MB-231 cells impaired TGFβ-mediated increase in *NEDD9* protein and mRNA levels (Fig. 5a,b). To assess whether *NEDD9* is also an MRTF target, we treated HCC1954 cells with cytochalasin-D (CD) and observed it increased *NEDD9* levels (Fig. 5c). *CTGF* and *Smad7* were used as controls. MDA-MB-231 cells treated with LB partially blocked TGFβ-mediated increased expression of *NEDD9* and several other MRTF-SRF target genes (*Fos*, *CTGF* and *Cyr61*). *FOSS* gene expression however was not affected (Fig. 5c). These results show that MRTF activity is necessary and sufficient to promote an increase in *NEDD9* levels.

ChIP-qPCR analysis within the *NEDD9* genomic locus (chr6:11,207,244–11,686,543) in MDA-MB-231 M1 showed strong TGFβ-induced binding of Smad2/3, SRF, MRTF-A and MRTF-B to intronic (R1 and R2) regions, and weak binding to the region 1 kb upstream of the short *NEDD9* transcript (R3) (Fig. 5d,e). Under similar experimental conditions, we were unable to detect Smad2/3 or SRF binding to the *NEDD9* locus in HCC1954 (data not shown). These data were confirmed by ChIP-sequencing in M1 MDA-MB-231 using a Smad2/3 antibody (Fig. 5f). These results show that in claudin<sup>low</sup> breast cancer cell lines TGFβ-mediated regulation

of *NEDD9* is achieved by Smad and MRTF-SRF binding within regulatory regions.

***NEDD9* mediates TGFβ-increased BTIC numbers.** We next asked whether *NEDD9* is required to mediate an expansion of BTICs. To test this, we first generated MDA-MB-231 constitutively expressing a short-hairpin RNA targeting *NEDD9* (MDA-MB-231-sh*NEDD9*) (Fig. 6a). MS-ICs and LDA assays showed TGFβ-mediated increases in both self-renewal activity and BTIC numbers were significantly lower in MDA-MB-231-sh*NEDD9* clones compared with control cells (Fig. 6b,c and Table 1). Moreover, forced overexpression of *NEDD9* in HCC1954 increased the number of MS-ICs by approximately twofold compared with vector control-treated cells, suggesting that an increase in *NEDD9* levels is sufficient to increase BTIC numbers (Fig. 6d).

***NEDD9* coordinates a positive feedback loop in claudin<sup>low</sup> cells.** We hypothesized *NEDD9* could, through its adaptor properties, be acting as a molecular scaffold to integrate TGFβ/Smad and MRTF-SRF signalling. Indeed, downregulation of *NEDD9* blocks TGFβ-mediated increase in Smad and SRF transcriptional activity (Fig. 6e,f). Moreover, SRF transcriptional activation of two of the three tested MRTF-SRF targets (*CTGF* and *CYR61*) was disrupted in sh-*NEDD9*-MDA-MB-231 mammosphere cultures at baseline

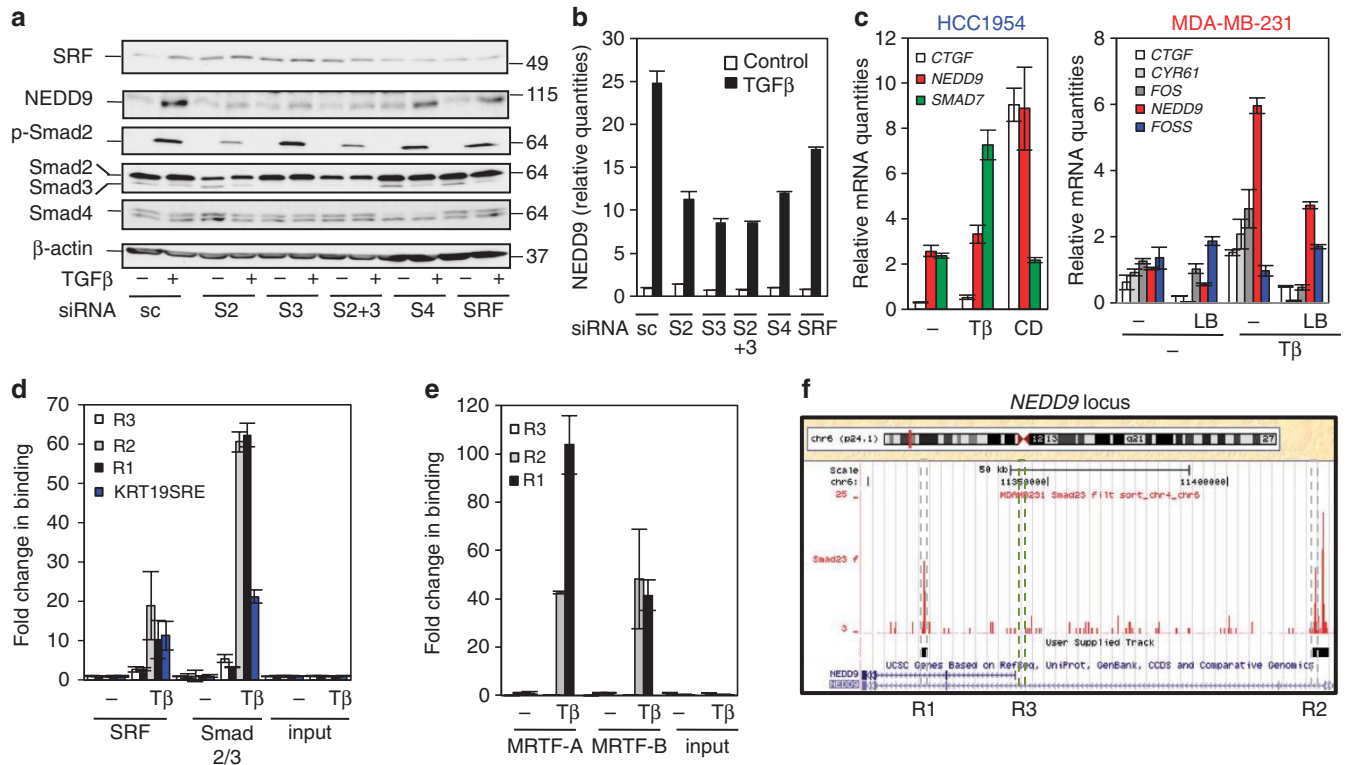


**Figure 5 | NEDD9 is a TGF $\beta$ /Smad and MRTF-SRF target.** (a) Western blot using the indicated antibodies of untreated (–) and TGF $\beta$  (2.5 ng ml $^{-1}$ )-treated (+) MDA-MB-231 M1 cultures transfected with siRNA pools against SRF, Smad2 (S2), Smad3 (S3) Smad2 and 3 (S2 + 3) and Smad4 (S4). (b) qRT-PCR analysis of *NEDD9* in same conditions as in (a). Error bars represent  $\pm$ s.d. of three experiments. (c) qRT-PCR of the indicated transcripts in HCC1954 (left panel) and MDA-MB-231 (right panel) M1 mammospheres treated with TGF $\beta$  (2.5 ng ml $^{-1}$ ), 5  $\mu$ M CD or 0.5  $\mu$ M LB as indicated. Expression was normalized against beta-2-microglobulin and expressed as arbitrary units. Error bars represent  $\pm$ s.d. of at least three independent experiments. (d) ChIP assay on MDA-MB-231 M1 mammospheres, untreated (–) or treated with TGF $\beta$  (2.5 ng ml $^{-1}$ ) (T $\beta$ ) for 1 h to detect binding of endogenous SRF and Smad2/3 to R1, R2 and R3. KRT19SBE region was used as an internal positive control for Smad2/3 binding. Results are expressed as TGF $\beta$ -induced fold change in binding from untreated control cultures. Error bars represent  $\pm$ s.d. of three independent experiments. (e) ChIP assay as described in (d) to detect binding of endogenous MRTF-A and MRTF-B. (f) UCSC Genome Browser display showing regions R1, R2 and R3 that were selected to design primers to detect binding of Smad, SRF, MRTF-A and MRTF-B by ChIP-qPCR assays. Error bars represent  $\pm$ s.d. of three independent experiments. Also showing ChIP-sequencing enrichment of Smad2/3 binding in M1 mammosphere cultures treated with TGF $\beta$  (2.5 ng ml $^{-1}$ ) for 1 h across the *NEDD9* genomic region. Black boxes correspond to called binding events obtained using both MACS and SWEMBL algorithms.

and after TGF $\beta$  treatment (Fig. 6g). Similarly, the levels of several TGF $\beta$ /Smad-specific downstream targets were diminished in sh-NEDD9-MDA-MB-231 compared with vector control cells in the presence of TGF $\beta$  (Fig. 6h). These results suggest that a positive feedback autoregulatory loop involving TGF $\beta$ -mediated regulation of NEDD9 enables both TGF $\beta$ /Smad and MRTF-SRF pathway activity to converge at specific regulatory regions, including those within the *NEDD9* genomic locus, to control the expression of a gene set involved in increasing BTIC numbers (Supplementary Fig. S6).

## Discussion

The results presented here represent a significant advance of our understanding of the dual role of the TGF $\beta$  pathway in regulating the growth and self-renewal of different subsets of normal and malignant mammary epithelial cells. We have identified a molecular mechanism where the NEDD9-Smad-SRF-dependent pathway regulates a TGF $\beta$ -specific transcriptional program (T $\beta$ SC-A) associated with human stem cell features, which is necessary for TGF $\beta$ -induced BTIC activity.

Previous observations showed TGF $\beta$  signalling has discordant effects on metastasis in mouse models<sup>41,42,43</sup>. Later, gene signatures specific of both active and inactive TGF $\beta$  pathway were correlated

with poor outcome in breast cancer patients<sup>44,45</sup>. We have reconciled these apparently conflicting results by characterizing TGF $\beta$  pathway response signatures in cancer stem cell-enriched cultures. We identified two independent signatures (T $\beta$ SC-A and T $\beta$ SC-B) associated with TGF $\beta$ -mediated increase and decrease in BTIC activity, respectively, and then tested these signatures in human breast tumours looking for associations with clinical outcome. We observed that only T $\beta$ SC-A is associated with a worse clinical outcome (and with stem cell features), showing that TGF $\beta$  prognostic signatures in breast cancer are ER-status independent, contrary to what was previously suggested<sup>44</sup>, but rather, associated with promotion of stem cell like features.

We show claudin<sup>low</sup> breast cancer cells are more likely than other breast cancer subtypes to respond to TGF $\beta$  treatment by increasing BTIC numbers, hence, we investigated TGF $\beta$  effects in different human normal mammary cell subpopulations, which are presumed to give rise to different breast cancer subtypes<sup>11,46</sup>. TGF $\beta$  signalling in the mammosphere-forming and migratory capacity of human normal mammary epithelial CD49f<sup>+</sup>EpcAM<sup>neg/low</sup> cells (where MaSCs reside) has been recently reported<sup>21</sup>. Our data expands these *in vitro* observations by using a more robust *in vivo* experimental approach<sup>30,31</sup>. We show a short (*ex vivo*) exposure to TGF $\beta$  increases *in vivo* MaSC/basal progenitor numbers independently of



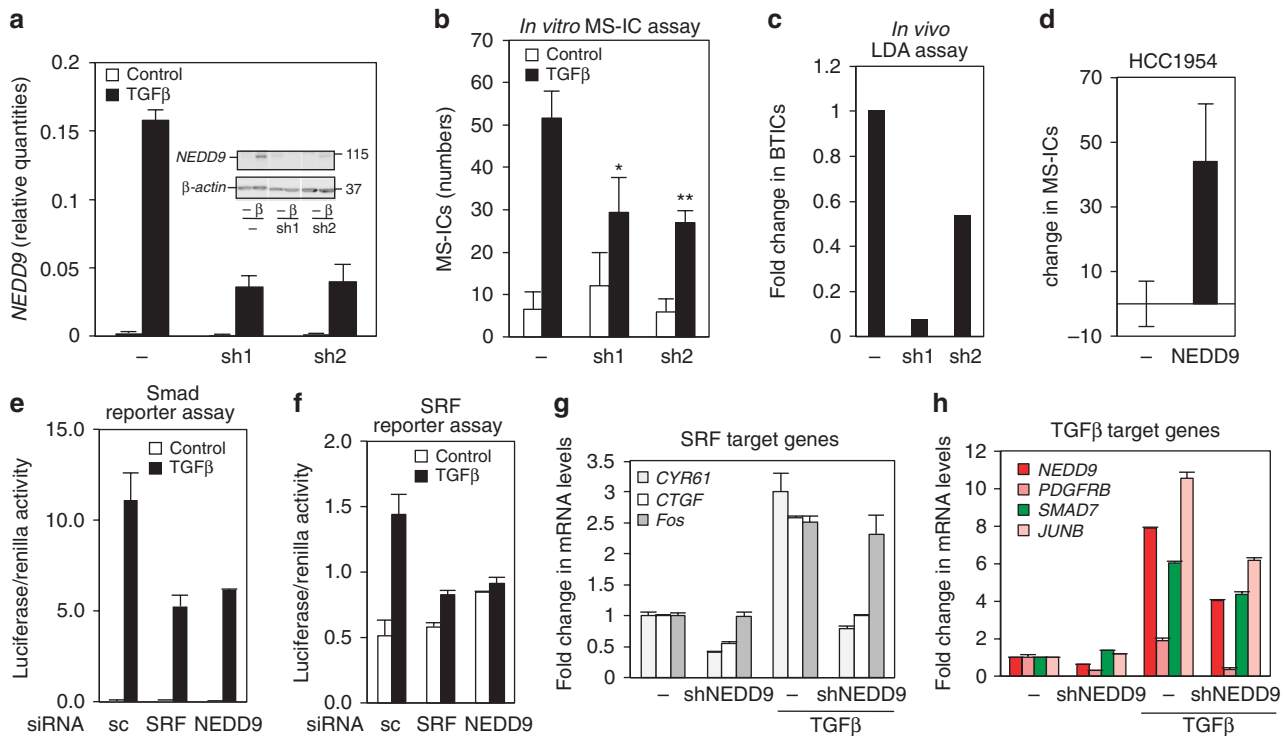


**Figure 6 | TGFβ-induced expansion of the BTIC pool requires NEDD9.** (a) qRT-PCR and western blot (insert) of NEDD9 in MDA-MB-231 transduced with empty vector control (-), or sh-NEDD9 (sh1 and sh2). NEDD9 expression was normalized against beta-2-microglobulin and expressed as arbitrary units. Error bars represent  $\pm$ s.d. of three independent experiments. (b) Bar chart shows number of MS-ICs in M1 cultures of MDA-MB-231 clones described in (a). Error bars represent  $\pm$ s.d. of at least three independent experiments. \*\*TGFβ-treated empty vector (-) cultures versus TGFβ-treated sh-NEDD9 cultures,  $P < 0.01$ . \*TGFβ-treated empty vector (-) cultures versus TGFβ-treated sh-NEDD9 cultures,  $P < 0.05$  (Student's *t*-test). (c) Bars represent TGFβ-induced fold change in total number of TICs in M1 cultures of MDA-MB-231-clones described in (a) as compared with untreated empty vector M1 cultures (-) (see Table 1). (d) A NEDD9 expression vector was transiently transduced into HCC1954 cells. Results show percentage of change in MS-IC numbers in NEDD9 overexpressing HCC1954 M1 mammospheres (NEDD9) compared with control transduced cells (-). Error bars represent  $\pm$ s.d. of independent experiments. (e) MDA-MB-231 cells were transfected in attached conditions with the indicated siRNAs and the TGFβ/Smad reporter vector (CAGA12-Luc). At 24 h post transfection, cells were passaged into a mammosphere culture and left untreated or treated with TGFβ ( $2.5 \text{ ng ml}^{-1}$ ) for further 20 h. Luciferase activity was normalized to pGL-SV40 renilla transfection control. Error bars represent  $\pm$ s.d. of three independent experiments. (f) MDA-MB-231 cells were transfected in attached conditions with the indicated siRNAs and the SRF reporter (p3DA.luc) and then treated as depicted in (d). Bar chart shows luciferase activity relative to renilla. Error bars represent  $\pm$ s.d. of three independent experiments. (g) qRT-PCR of downstream target genes of SRF and (h) TGFβ/Smad signalling pathways in M1 MDA-MB-231 transduced with empty vector control (-) or sh-NEDD9 (shNEDD9) left untreated or treated with TGFβ ( $2.5 \text{ ng ml}^{-1}$ ) for 1 h. Expression of mRNAs was normalized against beta-2-microglobulin and expressed as arbitrary units. Bars represent fold change in mRNA levels as compared with untreated empty vector transduced cells. Error bars represent  $\pm$ s.d. of three independent experiments.

its cytostatic effects in the CD49f<sup>+</sup>EpCAM<sup>neg/low</sup> compartment and decreases the clonogenic capacity of luminal-restricted progenitors within the CD49f<sup>+</sup>EpCAM<sup>+</sup> compartment. These results show conservation between TGFβ effects in breast cancer and normal cell subtypes.

TGFβ is a well-characterized EMT-inducing factor<sup>47</sup>. Because normal and malignant mammary stem cells show features of EMT and cells that have undergone EMT show properties of stem cells, the accepted model is that EMT and stemness are interlinked phenotypes<sup>21,22,48</sup>. Our observations show that TGFβ effects in BTIC are separable from EMT, as we observed TGFβ decreased BTIC activity in a basal-like cell line, and also mediated the induction of both EMT and an increase in the percentage of cells with a CD44<sup>+</sup>/CD24<sup>-</sup> phenotype. These results suggest mechanisms involved in TGFβ-induced changes on BTIC numbers are separable from those involved in promoting EMT and the CD44<sup>+</sup>/CD24<sup>-</sup> phenotype.

We found active SRF is required for TGFβ-mediated regulation of TβSC-A genes. Two main families of SRF co-factors have been characterized: members of the ternary complex factor family activated by mitogen-activated protein kinase phosphorylation

and members of the MRTF cofactors regulated by Rho-actin-dependent signals<sup>49</sup>. We focused on the Rho-actin-MRTF pathway for several reasons including that Smads had previously been shown to interact with MRTFs<sup>50</sup>, the Rho activity is induced by TGFβ in the claudin<sup>low</sup> MDA-MB-231 cell line but not in the basal HCC1954 cell line and also because others had shown in MDA-MB-231s SRF activity is regulated by Rho-actin-MRTF signals<sup>40</sup>. We dissected this pathway with the use of actin-modifiers, small-molecule inhibitors and siRNA technology and demonstrated that TGFβ-mediated effects on BTICs are dependent on Rho-actin-MRTF-SRF signalling.

A functional cross-talk between the TGFβ pathway and NEDD9 had been previously described<sup>17,51-53</sup>. NEDD9 is also known to be an MRTF target and to regulate a member of the Rho-family of GTPases through the Rac guanine nucleotide exchange factor DOCK3 (refs 40,54). This suggests the existence of a functional cross-talk between NEDD9 and the Rho-actin-MRTF-SRF pathway as well. Here we show the ability of TGFβ to induce NEDD9 is both Smad and actin-MRTF-SRF-dependent, only in claudin<sup>low</sup> cancer cells. Moreover, we observe NEDD9 is required for TGFβ-induced Smad and SRF activity. Altogether, this data leads us to hypothesize

that NEDD9, through a positive feedback loop, acts as a scaffold enabling the appropriate molecular interactions to connect TGF $\beta$ /Smad and Rho-actin-MRTF-SRF signals to coordinate the expression of genes involved in the expansion of the BTICs (Supplementary Fig. S6). We observed *NEDD9* was exclusively expressed in the human and mouse basal progenitor/MaSC populations, suggesting that the NEDD9 autoregulatory loop is also active in normal epithelial subpopulations and mediates TGF $\beta$ -dependent increase in epithelial stem cell numbers.

Interestingly in MDA-MB-231, a claudin<sup>low</sup> cell line, MRTF-SRF transcriptional activation of several target genes was previously shown to be required for experimental metastasis<sup>40</sup>. Our data now reveals their transcriptional regulation by SRF is important in the maintenance of BTICs. Therefore, we propose that therapeutic targeting of both Rho family GTPases and TGF $\beta$  signalling might be an attractive strategy to eliminate breast cancer metastasis in claudin<sup>low</sup> breast cancers, by both suppressing the spreading of cancer cells and the self-renewal of the BTIC population.

## Methods

**M1 mammosphere cultures.** Cells were processed to single-cell suspension from adherent cultures by trypsinization and cells were subsequently washed twice with PBS. A further wash in supplemented MEBM media was followed by filtration through a 40- $\mu$ m cell strainer. Single cells were plated on ultra-low attachment plates (Corning) at a density of 50,000 cells ml<sup>-1</sup> in supplemented MEBM media and grown for 7 days untreated or treated as indicated. M1 mammospheres were processed to single-cell suspension by trypsinization followed by neutralization using soyabean trypsin inhibitor 50  $\mu$ g ml<sup>-1</sup> (Roche). Cells were washed in PBS and resuspended in the same volume of supplemented MEBM as the initial primary mammosphere culture in the absence of treatment.

**MS-IC and CFC Assays.** For the MS-IC assay, the same number of single cells from the indicated cell lines were grown as M1 mammospheres for 7 days and left untreated or treated with single dose of TGF $\beta$  (2.5 ng ml<sup>-1</sup>) and/or of SB (10  $\mu$ M) as indicated. Next, all single cells from these M1 cultures were grown in the absence of treatment as M2 mammospheres and total number of spheres counted 7–10 days later. CFC assay: same number of single cells from the indicated cell lines were grown as M1 mammospheres untreated or treated with TGF $\beta$  (2.5 ng ml<sup>-1</sup>) and/or of SB (10  $\mu$ M) for 7 days as indicated. Aliquots of 100  $\mu$ l from processed M1 cultures were plated onto collagen-coated plates (Iwaki cell biology) in 4 ml of CFC media (DMEM:F12 medium (Invitrogen) with 5% fetal bovine serum, 5  $\mu$ g ml<sup>-1</sup> insulin (Sigma) and 20  $\mu$ g ml<sup>-1</sup> of human recombinant epidermal growth factor (Invitrogen)). Colony growth was monitored, and plates fixed and stained with acetone/methanol (1:1) and Giemsa once colonies reached sufficient size to be counted with the naked eye.

For the Limiting Dilution Assay, single cells from processed M1 cultures were encapsulated in 20  $\mu$ l gels; 7.8 parts 5:1 rat tail collagen:matrigel (Becton Dickinson), 2 parts 5 $\times$ DMEM (Invitrogen) 0.2 parts 1 M NaOH (Sigma). Gels containing specific cell numbers were implanted under general anaesthesia into the inguinal mammary glands of NOD/SCID *Il2rg*<sup>-/-</sup> (NSG) mice. Tumour growth was monitored by luciferase imaging on the IVIS imaging system (Caliper life sciences) and manual palpation.

**Chromatin Immunoprecipitation.** Single-cell suspensions of volume 125 ml at a density of 1 $\times$ 10<sup>5</sup> cells per ml were incubated with stirring in disposable spinner flasks (Corning) for 4 days at 37°C. Cell suspensions were treated with TGF $\beta$  for 1 h at 37°C, where indicated, and ChIP was performed following the method outlined in Schmidt *et al.*<sup>55</sup>, using SRF rabbit polyclonal antibody (Santa Cruz Biotechnology Inc. sc-335 X) and smad2/3 rabbit polyclonal antibody (Santa Cruz Biotechnology Inc. sc-8332 X) and Protein G Dynabeads (Dyna).

**Dissociation and cell separation of human mammary tissue.** The use of human material followed protocols approved by the Research Ethics Committee. We collected tissue from women undergoing reduction mammoplasty surgery with informed consent and processed the tissue as previously described<sup>56</sup>. Cell sorting was performed as previously described with some minor modifications<sup>56</sup>. Briefly, we preblocked mammary cell suspensions in 1 ml of cold HF (Hanks (+Mg +Ca) + 2% HEPES + 2% fetal bovine serum) supplemented with 10% normal rat serum, and then labelled them with an allophycocyanin-conjugated rat antibody to human CD49f (clone GOH3, R&D Systems) and PE-conjugated antibody to human EpCAM PE (clone 9C4, Biologend). We also labelled hematopoietic and endothelial cells with biotin-conjugated mouse antibodies to human CD45 (clone HI30, Biologend) and human CD31 (clone WM59, eBiosciences), respectively, followed by R-phycoerythrin-conjugated streptavidin (BD Biosciences). We added propidium iodide (Sigma) at 1 mg ml<sup>-1</sup> for live/dead cell discrimination. We performed all sorts on the FACS aria SORP (Becton Dickinson).

**Dissociation and cell separation of mouse mammary tissue.** Mammary glands from 8- to 14-week-old virgin female FVB mice were digested for 8 h at 37°C in DMEM/F12 (Gibco: with L-glut and Hepes) with 300 U ml<sup>-1</sup> collagenase and 100 U ml<sup>-1</sup> hyaluronidase (Sigma). After vortexing and lysis of the red blood cells in NH<sub>4</sub>Cl, a single-cell suspension was obtained by sequential dissociation of the fragments by gentle pipetting for 1–2 min in 0.25% trypsin, and then 2 min in 5 mg ml<sup>-1</sup> dispase II plus 0.1 mg ml<sup>-1</sup> DNase I (Sigma). Cell separation was performed as previously described<sup>32</sup>. Briefly, cells were incubated for 10 min at 4°C in 10% rat serum and stained with CD45-biotin (clone 30-F11 eBioscience), CD31-biotin (clone 390 eBioscience), Ter119-biotin (Ter119 eBioscience), BP-1-biotin, (Pharmingen), CD49f-AF488 (clone GoH3 Biologend) and EpCAM-AF647 (clone G8.8 Biologend). Cell death was determined by DAPI staining.

**Analysis of claudin<sup>low</sup> score in cell lines and tumour samples.** We used the cell line expression data from Neve *et al.*<sup>57</sup> and the nine-cell line claudin<sup>low</sup> signature from Prat *et al.*<sup>9</sup> to obtain a claudin<sup>low</sup> centroid and an 'others' centroid, following the methodology in that paper<sup>9,57</sup>. Then, we normalized Illumina microarray data from the 11 cell lines analysed by us using beadarray<sup>58</sup> and annotated the probes using the latest files available in the re-annotation pipeline from Barbosa-Morais *et al.*<sup>59</sup>, finding 741 of their signature genes in our arrays. With those genes, we computed the Spearman correlation of our cell lines to each of the centroids. The Claudin<sup>low</sup> score is the difference of the Spearman correlation value of our cell line expression data with the claudin<sup>low</sup> centroid and the Spearman correlation with the 'others' centroid (positive values indicate more Spearman correlation with the claudin<sup>low</sup> centroid and negative values more Spearman correlation with the 'others' centroid). We used Spearman correlation instead of Euclidean distance, as Prat *et al.*<sup>9</sup> did, because it is a more robust measure when dealing with expression levels of different microarray platforms. We employed the same methodology on the claudin<sup>low</sup> tumour predictor of Prat *et al.*<sup>9</sup> to classify the Metabric set of 997 breast tumours<sup>36</sup>, with 104 tumours classified as claudin<sup>low</sup>.

**Gene set enrichment analysis.** We ran GSEA v 2.07.34 on our Metabric data set to test if T $\beta$ SC-A signature is enriched in the claudin<sup>low</sup> tumours. As GSEA does not support gene sets that have both up- and downregulated genes, we used the subset of overexpressed genes in T $\beta$ SC-A. For genes spanning several probes, we selected the best-annotated probe or the one showing more variability. The number of signature genes present in the Metabric microarray was 43.

**Regulatory network analysis.** ECRbase was used as the resource for TF-binding site annotation (see Supplementary Information). We selected the subset of annotated TF-binding site that are conserved in human-opsom ECRs in the 5 Kb immediately upstream of the transcription start site. Thus, binding profiles for each position weight matrix (PWM) over all human ENSEMBL genes was constructed with a '1' indicating presence of motif in 5 Kb promoter region upstream of the gene, '0' otherwise. ENSEMBL IDs were mapped to Entrez Gene Ids. Next, for each TGF $\beta$  versus SB comparison, we extracted the regularized *t*-statistics of differential expression. Probes were mapped to Entrez Gene Ids and the *t*-statistics regressed against the binding profile of a PWM in a linear model<sup>39</sup> of the form *t*-statistics (TGF $\beta$  versus SB) =  $\alpha \cdot P_{PWM} + \epsilon$ , from which a *P*-value of significance was derived. PWMs were then ranked according to significance of these *P*-values. Histogram of *P*-values showed skews towards small *P*-values suggesting significant differential activity of PWMs in response to TGF $\beta$  treatment.

**Plurinet analysis.** Genes from the plurinet network<sup>35</sup> were mapped to the Illumina array using Entrez ID identifiers and fold-change (FC) values (TGF $\beta$  versus SB) were extracted for each cell line. Next, we selected those that showed at least 1.25 FCs in either the two T $\beta$ SC-A or T $\beta$ SC-B cell lines, and only considered those where the direction of the FC was consistent between the two cell lines. The relaxation of the threshold to  $\pm 1.25$  was justified based on the observation that the 'Plurinet' itself was derived from an algorithm that only demanded consistent directional changes over a local protein-protein interaction subnetwork without requiring the individual changes to be significant. Thus, for each set of cell lines, we could count the number of 'Plurinet' genes showing increases and decreases in TGF $\beta$  versus SB conditions. Any trend towards up- or downregulation of 'Plurinet' genes in the cell lines with TGF $\beta$ -induced BCSC activity against the other two cell lines could then be evaluated using a Fisher's exact test.

## References

- Al-Hajj, M., Wicha, M. S., Benito-Hernandez, A., Morrison, S. J. & Clarke, M. F. Prospective identification of tumorigenic breast cancer cells. *Proc. Natl Acad. Sci. USA* **100**, 3983–3988 (2003).
- Collins, A. T., Berry, P. A., Hyde, C., Stower, M. J. & Maitland, N. J. Prospective identification of tumorigenic prostate cancer stem cells. *Cancer Res.* **65**, 10946–10951 (2005).
- Ricci-Vitiani, L. *et al.* Identification and expansion of human colon-cancer-initiating cells. *Nature* **445**, 111–115 (2007).
- O'Brien, C. A., Pollett, A., Gallinger, S. & Dick, J. E. A human colon cancer cell capable of initiating tumour growth in immunodeficient mice. *Nature* **445**, 106–110 (2007).

5. Ginestier, C. *et al.* ALDH1 is a marker of normal and malignant human mammary stem cells and a predictor of poor clinical outcome. *Cell Stem Cell* **1**, 555–567 (2007).
6. Perou, C. M. *et al.* Molecular portraits of human breast tumours. *Nature* **406**, 747–752 (2000).
7. Sorlie, T. *et al.* Gene expression patterns of breast carcinomas distinguish tumor subclasses with clinical implications. *Proc. Natl Acad. Sci. USA* **98**, 10869–10874 (2001).
8. Hennessy, B. T. *et al.* Characterization of a naturally occurring breast cancer subset enriched in epithelial-to-mesenchymal transition and stem cell characteristics. *Cancer Res.* **69**, 4116–4124 (2009).
9. Prat, A. *et al.* Phenotypic and molecular characterization of the claudin-low intrinsic subtype of breast cancer. *Breast Cancer Res.* **12**, R68 (2010).
10. Proia, T. A. *et al.* Genetic predisposition directs breast cancer phenotype by dictating progenitor cell fate. *Cell Stem Cell* **8**, 149–163 (2011).
11. Lim, E. *et al.* Aberrant luminal progenitors as the candidate target population for basal tumor development in BRCA1 mutation carriers. *Nat Med* **15**, 907–913 (2009).
12. Stingl, J. & Caldas, C. Molecular heterogeneity of breast carcinomas and the cancer stem cell hypothesis. *Nat. Rev. Cancer* **7**, 791–799 (2007).
13. Massagué, J. TGFbeta in Cancer. *Cell* **134**, 215–230 (2008).
14. Bierie, B. & Moses, H. L. Tumour microenvironment: TGFbeta: the molecular Jekyll and Hyde of cancer. *Nat. Rev. Cancer* **6**, 506–520 (2006).
15. Dumont, N. & Arteaga, C. L. Targeting the TGF beta signaling network in human neoplasia. *Cancer Cell* **3**, 531–536 (2003).
16. Bierie, B. & Moses, H. L. Gain or loss of TGFbeta signaling in mammary carcinoma cells can promote metastasis. *Cell Cycle* **8**, 3319–3327 (2009).
17. Padua, D. *et al.* TGFbeta primes breast tumors for lung metastasis seeding through angiopoietin-like 4. *Cell* **133**, 66–77 (2008).
18. Bierie, B. *et al.* Abrogation of TGF-beta signaling enhances chemokine production and correlates with prognosis in human breast cancer. *J. Clin. Invest.* **119**, 1571–1582 (2009).
19. Nishimura, E. K. *et al.* Key roles for transforming growth factor beta in melanocyte stem cell maintenance. *Cell Stem Cell* **6**, 130–140 (2010).
20. Ikushima, H. *et al.* Autocrine TGF-beta signaling maintains tumorigenicity of glioma-initiating cells through Sry-related HMG-box factors. *Cell Stem Cell* **5**, 504–514 (2009).
21. Scheel, C. *et al.* Paracrine and autocrine signals induce and maintain mesenchymal and stem cell States in the breast. *Cell* **145**, 926–940 (2011).
22. Mani, S. A. *et al.* The epithelial-mesenchymal transition generates cells with properties of stem cells. *Cell* **133**, 704–715 (2008).
23. Shipitsin, M. *et al.* Molecular definition of breast tumor heterogeneity. *Cancer Cell* **11**, 259–273 (2007).
24. Tang, B. *et al.* Transforming growth factor-beta can suppress tumorigenesis through effects on the putative cancer stem or early progenitor cell and committed progeny in a breast cancer xenograft model. *Cancer Res.* **67**, 8643–8652 (2007).
25. Dontu, G. *et al.* *In vitro* propagation and transcriptional profiling of human mammary stem/progenitor cells. *Genes Dev.* **17**, 1253–1270 (2003).
26. Stingl, J., Eaves, C. J., Zandieh, I. & Emerman, J. T. Characterization of bipotent mammary epithelial progenitor cells in normal adult human breast tissue. *Breast Cancer Res. Treat* **67**, 93–109 (2001).
27. Xu, Y. D. *et al.* Release of biologically active TGF-beta1 by alveolar epithelial cells results in pulmonary fibrosis. *Am. J. Physiol. Lung Cell Mol. Physiol.* **285**, L527–539 (2003).
28. Siegel, P. M., Shu, W., Cardiff, R. D., Muller, W. J. & Massagué, J. Transforming growth factor beta signaling impairs Neu-induced mammary tumorigenesis while promoting pulmonary metastasis. *Proc. Natl Acad. Sci. USA* **100**, 8430–8435 (2003).
29. Stingl, J., Eaves, C. J., Zandieh, I. & Emerman, J. T. Characterization of bipotent mammary epithelial progenitor cells in normal adult human breast tissue. *Breast Cancer Res. Treat.* **67**, 93–109 (2001).
30. Eirew, P. *et al.* A method for quantifying normal human mammary epithelial stem cells with *in vivo* regenerative ability. *Nat. Med.* **14**, 1384–1389 (2008).
31. Eirew, P., Stingl, J. & Eaves, C. J. Quantitation of human mammary epithelial stem cells with *in vivo* regenerative properties using a subrenal capsule xenotransplantation assay. *Nat. Protoc.* **5**, 1945–1956 (2010).
32. Stingl, J. *et al.* Purification and unique properties of mammary epithelial stem cells. *Nature* **439**, 993–997 (2006).
33. Kalkhoven, E. *et al.* Resistance to transforming growth factor beta and activin due to reduced receptor expression in human breast tumor cell lines. *Cell Growth Differ.* **6**, 1151–1161 (1995).
34. Subramanian, A. *et al.* Gene set enrichment analysis: a knowledge-based approach for interpreting genome-wide expression profiles. *Proc. Natl Acad. Sci. USA* **102**, 15545–15550 (2005).
35. Müller, F.-J. *et al.* Regulatory networks define phenotypic classes of human stem cell lines. *Nature* **455**, 401–405 (2008).
36. Curtis, C. *et al.* The genomic and transcriptomic architecture of 2,000 breast tumours reveals novel subgroups. *Nature* **486**, 346–352 (2012).
37. Pece, S. *et al.* Biological and molecular heterogeneity of breast cancers correlates with their cancer stem cell content. *Cell* **140**, 62–73 (2010).
38. Bussemaker, H. J., Li, H. & Siggia, E. D. Regulatory element detection using correlation with expression. *Nat. Genet.* **27**, 167–171 (2001).
39. Gao, F., Foat, B. C. & Bussemaker, H. J. Defining transcriptional networks through integrative modeling of mRNA expression and transcription factor binding data. *BMC Bioinformatics* **5**, 31 (2004).
40. Medjkane, S., Perez-Sanchez, C., Gaggioli, C., Sahai, E. & Treisman, R. Myocardin-related transcription factors and SRF are required for cytoskeletal dynamics and experimental metastasis. *Nat. Cell Biol.* **11**, 257–268 (2009).
41. Muraoka, R. S. *et al.* Increased malignancy of Neu-induced mammary tumors overexpressing active transforming growth factor beta1. *Mol. Cell Biol.* **23**, 8691–8703 (2003).
42. Siegel, P. M., Shu, W., Cardiff, R. D., Muller, W. J. & Massague, J. Transforming growth factor beta signaling impairs Neu-induced mammary tumorigenesis while promoting pulmonary metastasis. *Proc. Natl Acad. Sci. USA* **100**, 8430–8435 (2003).
43. Forrester, E. *et al.* Effect of conditional knockout of the type II TGF-beta receptor gene in mammary epithelia on mammary gland development and polyomavirus middle T antigen induced tumor formation and metastasis. *Cancer Res.* **65**, 2296–2302 (2005).
44. Padua, D. *et al.* TGFbeta primes breast tumors for lung metastasis seeding through angiopoietin-like 4. *Cell* **133**, 66–77 (2008).
45. Bierie, B. *et al.* Transforming growth factor-beta regulates mammary carcinoma cell survival and interaction with the adjacent microenvironment. *Cancer Res.* **68**, 1809–1819 (2008).
46. Prat, A. & Perou, C. M. Mammary development meets cancer genomics. *Nat. Med.* **15**, 842–844 (2009).
47. Ofi, M. *et al.* TGF-beta1 and Ha-Ras collaborate in modulating the phenotypic plasticity and invasiveness of epithelial tumor cells. *Genes Dev.* **10**, 2462–2477 (1996).
48. Taube, J. H. *et al.* Core epithelial-to-mesenchymal transition interactome gene-expression signature is associated with claudin-low and metaplastic breast cancer subtypes. *Proc. Natl Acad. Sci. USA* **107**, 15449–15454 (2010).
49. Posern, G. & Treisman, R. Actin 'together': serum response factor, its cofactors and the link to signal transduction. *Trends Cell Biol.* **16**, 588–596 (2006).
50. Morita, T., Mayanagi, T. & Sobue, K. Reorganization of the actin cytoskeleton via transcriptional regulation of cytoskeletal/focal adhesion genes by myocardin-related transcription factors (MRTFs/MAL/MKLS). *Exp. Cell Res.* **313**, 3432–3445 (2007).
51. Vogel, T., Ahrens, S., Büttner, N. & Kriegstein, K. Transforming growth factor beta promotes neuronal cell fate of mouse cortical and hippocampal progenitors *in vitro* and *in vivo*: identification of Nedd9 as an essential signaling component. *Cereb. Cortex* **20**, 661–671 (2010).
52. Zheng, M. & McKeown-Longo, P. J. Regulation of HEF1 expression and phosphorylation by TGF-beta 1 and cell adhesion. *J. Biol. Chem.* **277**, 39599–39608 (2002).
53. Giampieri, S. *et al.* Localized and reversible TGFbeta signalling switches breast cancer cells from cohesive to single cell motility. *Nat. Cell Biol.* **11**, 1287–1296 (2009).
54. Sanz-Moreno, V. *et al.* Rac activation and inactivation control plasticity of tumor cell movement. *Cell* **135**, 510–523 (2008).
55. Schmidt, D. *et al.* ChIP-seq: using high-throughput sequencing to discover protein-DNA interactions. *Methods* **48**, 240–248 (2009).
56. Eirew, P. *et al.* A method for quantifying normal human mammary epithelial stem cells with *in vivo* regenerative ability. *Nat. Med.* **14**, 1384–1389 (2008).
57. Neve, R. M. *et al.* A collection of breast cancer cell lines for the study of functionally distinct cancer subtypes. *Cancer Cell* **10**, 515–527 (2006).
58. Dunning, M. J., Smith, M. L., Ritchie, M. E. & Tavare, S. beadarray: R classes and methods for Illumina bead-based data. *Bioinformatics* **23**, 2183–2184 (2007).
59. Barbosa-Morais, N. L. *et al.* A re-annotation pipeline for Illumina BeadArrays: improving the interpretation of gene expression data. *Nucleic Acids Res.* **38**, e17 (2010).

## Acknowledgements

We would like to acknowledge the support of The University of Cambridge, Cancer Research UK and Hutchison Whampoa Limited, the NIHR Cambridge Biomedical Research Centre, all the people that provided us with reagents (see Supplementary Information), the SEARCH study team and the Core facilities at the Cambridge Research Institute. This work was supported by Cancer Research UK. A.B. was a Marie Curie (IEF) fellow in 2010 and 2011. AT is supported by a Heller Research Fellowship.

## Author contributions

A.B. and C.C. conceived the project, designed and oversaw experiments. A.B., W.G., J.L.S. and A.T.V. generated data. A.S. and J.S. together with A.B. performed the mouse experiments. A.T. and D.M.S. performed GSEA, Kaplan–Meier and regulatory network analysis with TβSC signatures. O.M.R. generated the analyses associated with the

claudin<sup>low</sup> signature and provided statistical expertise. J.L.Q and P.P. generated and analysed the p-Smad2. A.B and C.C. wrote the manuscript. C.C. is the senior author.

### Additional information

**Accession codes:** Microarray data have been deposited in ArrayExpress under the accession codes E-MTAB-516 and E-MTAB-1190.

**Supplementary Information** accompanies this paper at <http://www.nature.com/naturecommunications>

**Competing financial interests:** The authors declare no competing financial interests.

**Reprints and permission** information is available online at <http://npg.nature.com/reprintsandpermissions/>

**How to cite this article:** Bruna, A. *et al.* TGF $\beta$  induces the formation of tumour-initiating cells in claudin<sup>low</sup> breast cancer. *Nat. Commun.* 3:1055 doi: 10.1038/ncomms2039 (2012).